JOURNAL OF AIRCRAFT
Vol. 29, No. 2, March–April 1992

Numerical Computation of Improved Transonic Potential Method

Zhu Zi-qiang* and Bai Xue-Song†
Beijing University of Aeronautics and Astronautics, Beijing, China

Several points concerning the transonic potential method are briefly reviewed. Comparison of two correction orders—the nonisentropic jump conditions and the vorticity generated behind the shock—shows that the vorticity correction is indeed of higher order. An entropy shock point operator is introduced to account for entropy correction. Numerical examples in two- and three-dimensional cases show that nonisentropic formulation can simulate inviscid flow better than the traditional potential method, and it has the advantage of simplicity in its mathematical aspects, as does the potential method.

Nomenclature

A = aspect ratio
a = velocity of sound
a^* = critical velocity of sound
M = Mach number
Re = Reynolds number
t = thickness of wing section
u = velocity
ρ = density
ω = under-relaxation parameter
α = angle of attack
χ = swept angle of 1/4 chord line

Subscript
∞ = freestream

Introduction

PROGRESS in the area of numerical computation of transonic flow has been startling, and the discipline now encompasses a range of separate and different activities. It is well known that a complete description of the transonic flowfield can only be obtained from the Navier-Stokes (N-S) equation. At present, it appears that computer codes based on the N-S equation will not be inexpensive nor routine for aerodynamic design purposes, due to computer limitations and lack of an accurate turbulence model, even though more and more numerical results of the solution of N-S equation have been arising. In high Reynolds number flow, the viscous/inviscid interaction method is reasonably inexpensive and has been widely used in industry. It is more complicated to solve the Euler equation, which describes accurately the inviscid flowfield, and the potential flow method can still be an order-of-magnitude faster and require less computer resources. Because engineering applications frequently require a large number of flow simulations before the optimum design configuration can be reached, fast and efficient methods are needed. It has made potential approximation a pre-eminent approach in the transonic range for the design and analysis of advanced commercial aircraft in the past five to ten years, although significant progress has also been made in numerical simulation of the Euler equation. Although results indicate that the traditional potential method does not accurately model the exact inviscid flow, it is worthwhile and attractive to attempt to improve the accuracy of this method. In this paper, several points concerning the potential method are briefly reviewed first, and then the formulation of a nonisentropic potential method and its numerical results are given.

Received June 26, 1989; revision received Sept. 2, 1990; accepted for publication Oct. 22, 1990.

*Professor of Applied Mechanics, 37 Xueyuan Road, Haidian District.

†Ph.D. Student, Department of Applied Mechanics, 37 Xueyuan Road, Haidian District.

Review of the Full Potential Method

The use of a potential equation rests on the assumption that the flow is isentropic, but whenever shock waves exist this ceases to be true. It is argued that the entropy rise through a shock wave is proportional to the third power of shock strength, which is measured by M^2-1, where M is the Mach number just ahead of the shock. Thus, the flow is expected only to be one with shock-free or fairly weak shock waves for the potential method. This is the main limitation for application of this method.

The development of a computational transonic potential flow equation in the past has included assessments of the effects of different numerical solution schemes. One remaining controversy is that of "fully conservative" vs "nonconservative" schemes.

The fully conservative scheme approximates an adequate weak solution and ensures the conservation of mass, whereas the nonconservative scheme makes no attempt to ensure mass or moment conservation. The amount of introduced mass and, hence, predicted shock by the numerical scheme can be expected to be nonunique and to vary with the local grid spacing.[1,2] This is the main weakness of a nonconservative solution. However, experience shows there is often better agreement with experimental results using the nonconservative solution.[3,4] Hence, the contradiction between theoretical rationality and accuracy of calculated results in practice is one of the problems of the potential method.

Multiple solution is another problem that occurs in numerical calculation of the full potential equation. The comparative study of the numerical results for two-dimensional steady flow indicates that the nonuniqueness problem is not inherent in inviscid flow, but rather a result of conservative isentropic potential approximation treatment of shock waves.[5,6] The comparative study[7] of numerical results for a two-dimensional unsteady small perturbation transonic equation indicates that at lower supercritical Mach number there is only one stable equilibrium solution. As Mach number increases, the original solution becomes unstable and two new stable solutions appear. Hence, nonuniqueness of steady state arises from the onset of instability in an equilibrium state, i.e., from a sensitivity of the final equilibrium to changes in the initial conditions. For example, for a NACA 0012 airfoil at zero angle of attack

there are three equilibrium flowfields at any Mach number between 0.835 and 0.858. The symmetric state is unstable, and two asymmetric states are stable. In such a case, the shocks cannot stand symmetrically on the upper and lower surfaces. The instability is essentially independent of the numerical scheme used, and, in fact, is a property of the differential equation. It is pointed out in Ref. 7 that a more persuasive argument can be made that the instabilities must arise in the Euler equations as well. In Ref. 8, it was also pointed out that there is no proof of an existing unique solution for steady Euler equations in the transonic regime. Further investigation of the reason for appearing multisolution is needed.

Entropy and Vorticity Correction

It is clear that, for high Mach number flows with shocks, the irrotationality assumption, which is the basic assumption in potential flow method, is questioned, and efforts are directed towards efficient methods to solve the transonic rotational flow by extending potential calculation, namely, the nonisentropic jump conditions and the vorticity generated behind the shock.

A comparison of the two correction orders determines that the vorticity effect is of a higher order than the entropy effect, a fact first described by Hayes,[9] and again by Hafez and Lovell.[10] Hence, it is feasible to account for the entropy only and neglect the vorticity. It is expected that such a nonisentropic formulation can simulate inviscid flow better than the traditional potential method, while retaining the advantage of mathematical simplicity of the traditional potential formulation.

Entropy Shock Point Operator

Neither the "conservative" nor the "nonconservative" scheme can correctly simulate jump conditions across shock waves. To improve this situation, Collyer and Lock[11] introduced a partially conservative scheme with an experimentally determined parameter λ. Recently, Metrens et al.[12] proposed a prop shock point operator. It satisfies the Prandtl relation, but is still nonconservative in mass conservation. Complementing all other results,[13-15] an entropy shock point operator was introduced[16,17] to account for entropy correction.

Assuming one-dimensional flow, for simplicity, we have

$$A := (\rho u)_x = 0 \tag{1}$$

At shock point i, the entropy shock point operator is

$$D^- A + DA + B = (\rho u)_{i+1/2} - (\rho u)_{i-3/2} + B = 0 \tag{2}$$

where

$$B = (K_s - 1)(\rho u)_{i+1/2}$$

$$K_s = \frac{u_{i-3/2}^2}{a_*^2} \left\{ \frac{1 + [(\gamma-1)/2] M_\infty^2 (1 - u_{i-3/2}^2)}{1 + [(\gamma-1)/2] M_\infty^2 (1 - u_{i+1/2}^2)} \right\}^{\frac{1}{(\gamma-1)}} \tag{3}$$

One can see that this shock point operator satisfies Prandtl's relation exactly—i.e., momentum conservation.[17] From Eq. (2)

$$K_s(\rho u)_{i+1/2} - (\rho u)_{i-3/2} = 0 \tag{4}$$

At first appearance, it is nonconservative in mass. But we can rewrite it as

$$(\rho_s u)_{i+1/2} - (\rho_s u)_{i-3/2} = 0 \tag{5}$$

where

$$\rho_s = \rho \cdot k_s = \left\{ k^{-1} \left[1 + \frac{\gamma - 1}{2} M_\infty^2 (1 - q^2) \right] \right\}^{\frac{1}{(\gamma-1)}}$$

$$k = \frac{1 + [(\gamma-1)/2] M_\infty^2 (1 - u_{i+1/2}^2)}{1 + [(\gamma-1)/2] M_\infty^2 (1 - u_{i-3/2}^2} \cdot \left(\frac{a_*^2}{u_{i-3/2}^2} \right)^{(\gamma-1)} \tag{6}$$

In front of shock wave, $K_s = 1$, $\rho_s = \rho$; behind shock wave, ρ_s actually is the density in nonisentropic sense, which satisfies the entropy increase relation according to the second law of thermodynamics. It is obvious that this shock point operator satisfies momentum conservation as well as mass conservation. The comparison of different shock point operators with the exact solution for the shock strength is given in Fig. 1. From this comparison, it can be seen that the entropy shock point operator is more appropriate than others.

Numerical Results and Discussion

For the steady uniform incoming flow, the upstream field in front of the shock wave is isentropic. Behind shock wave, the flowfield is not isentropic, but along a streamline the value of entropy is constant. Values at grid points over the whole field behind shock can be obtained by interpolation in computational space. The shock strengths on the upper and lower wing surfaces generally are different, and so it is also necessary to modify the wake condition in computation.[17] Some typical numerical results of nonisentropic potential method in both two and three dimensions are given below.

Results of the Calculation in the Two-Dimensional Case

The conservative nonisentropic full potential equation is solved by using the type of AF2 scheme described in Ref. 18, which is similar to Holst's "TAIR."[19] In computation, the O-type grid generated by conformal mapping is used, and grid points 64×17 are adopted. The computational example has demostrated[16] that the results of the nonisentropic potential method are closer to both the Euler solution and the experimental data than the results of traditional isentropic potential method, while its computational efforts are comparable to the usual isentropic potential method, i.e., the CPU time and the computer resources required are much less than for the Euler solution. Figure 2 shows the pressure distribution of two airfoils. Curve C_l vs α of a NACA 0012 airfoil at $M_\infty = 0.83$ is depicted in Fig. 3 (superimposed on a figure from Ref. 7). In this example, the isentropic conservative potential solution is not unique. The nonisentropic model produces, however, a unique solution. It seems the nonuniqueness problem is circumvented at least for this numerical example.

Viscous transonic airfoil flow simulation is one of the important tasks in aeronautical industry application. A viscous-inviscid interaction method, in which zonal solutions for the inviscid and viscous flow region are iteratively matched, was given in Ref. 20 to simulate viscous airfoil flow. The nonisentropic full-potential flow method and inverse boundary-layer

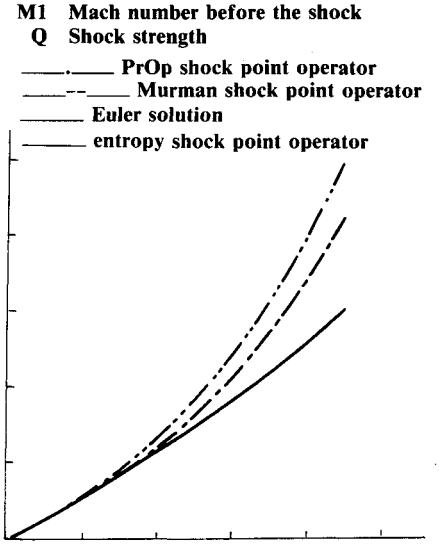

Fig. 1 Comparison of shock point operator.

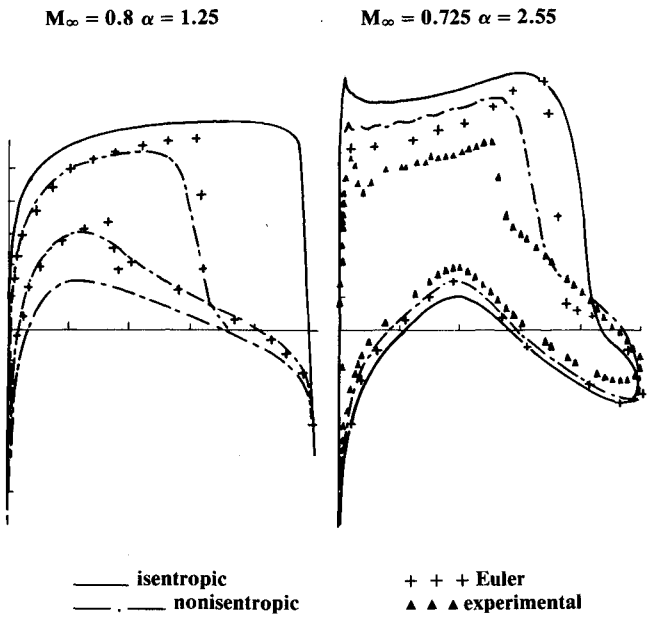

Fig. 2 Pressure distribution around NACA 0012 and RAE 2822 airfoils (inviscid).

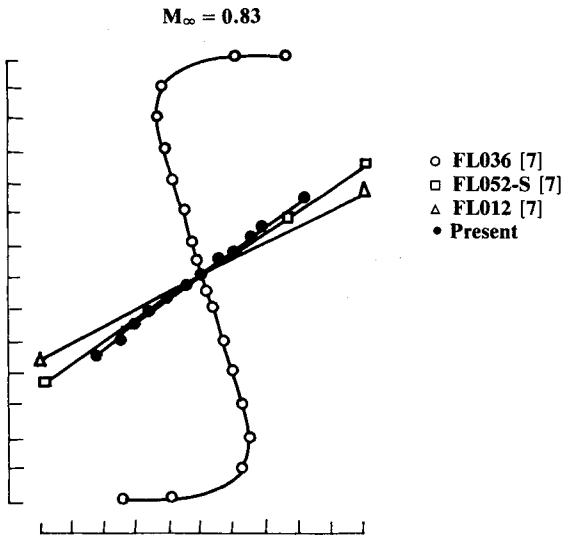

Fig. 3 Lift characteristics of NACA 0012.

method[21] are alternatively used as inviscid and viscous solutions, combined with semi-inverse coupling as the final solution of viscous transonic flow around an airfoil. The inviscid iterative solution is interrupted periodically to solve the boundary-layer integral equations and to update the boundary conditions using an under-relaxation. The value of the constant relaxation parameter ω has to be evaluated by numerical tests. In our numerical investigations, which we updated after every 16-24 inviscid cycles, we used an under-relaxation of $\omega = 0.3$-0.6 for different cases, depending on the extent of separated region. To assure convergence for massive separated flows, small values of ω are needed. In Fig. 4, the calculated pressure distribution is compared with experimental data for a NACA 0012 airfoil at $M_\infty = 0.753$, $\alpha = 2.26$ deg, and for an RAE 2822 airfoil at $M_\infty = 0.73$, $\alpha = 2.56$ deg. For comparison purposes, the calculated results of the isentropic potential method are also given in the figure. From the comparison, it is evident that the nonisentropic potential results, including the viscous effect, agree well with the experimental data.

Results of the Calculation in the Three-Dimensional Case

Noting the results of the two-dimensional case, it seems worthwhile to apply the same formulation to the three-dimensional case. In the three-dimensional calculation, the full-potential equation is solved by the improved multigrid transonic potential solver E92BM, which was obtained by modifying FLO27M with the externally formed C-O grid instead of with the original mapping-formed C-H grid. The grid type O-O offers the most efficiency in terms of computational work for a given resolution, since it gives the greatest density of grid points around the wing for a given total number of grid points.

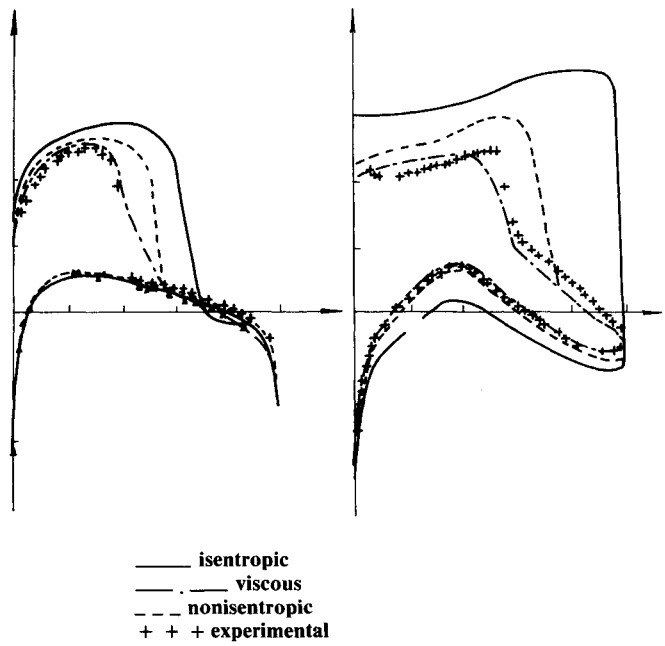

Fig. 4 Pressure distribution around NACA 0012 and RAE 2822 airfoils (viscous).

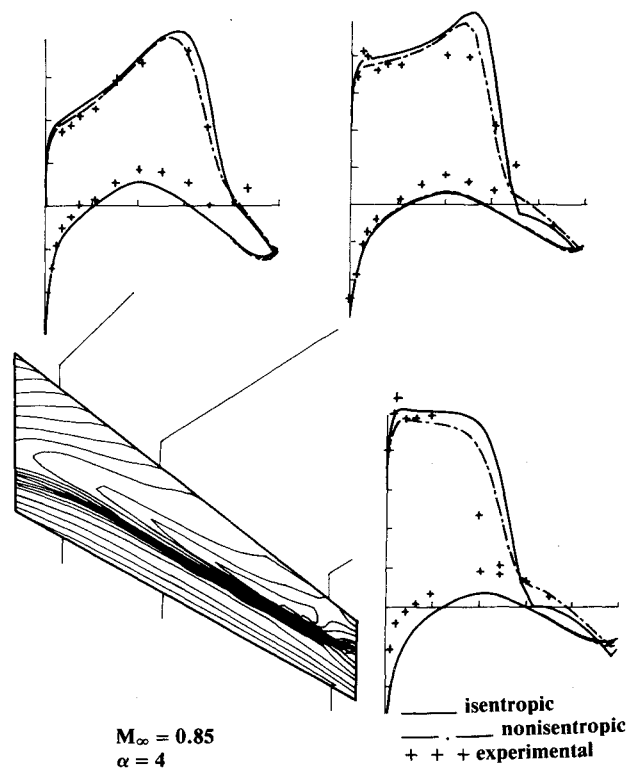

Fig. 5 Isobars and pressure distribution at some spanwise stations around a swept wing.

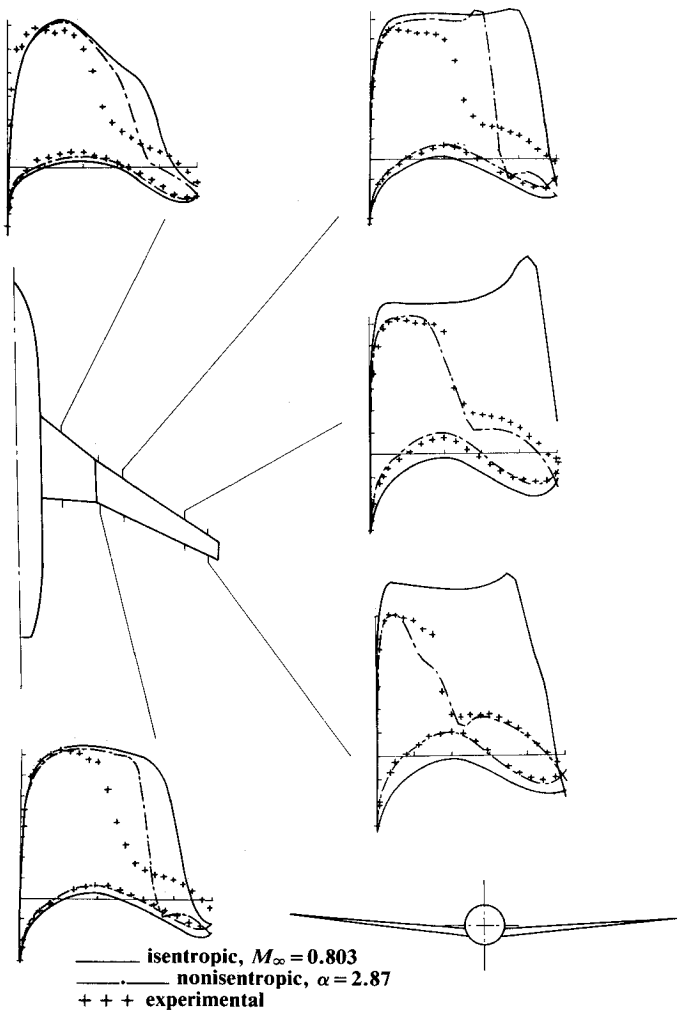

Fig. 6 Comparison of pressure distribution at some stations around a wing-body combination.

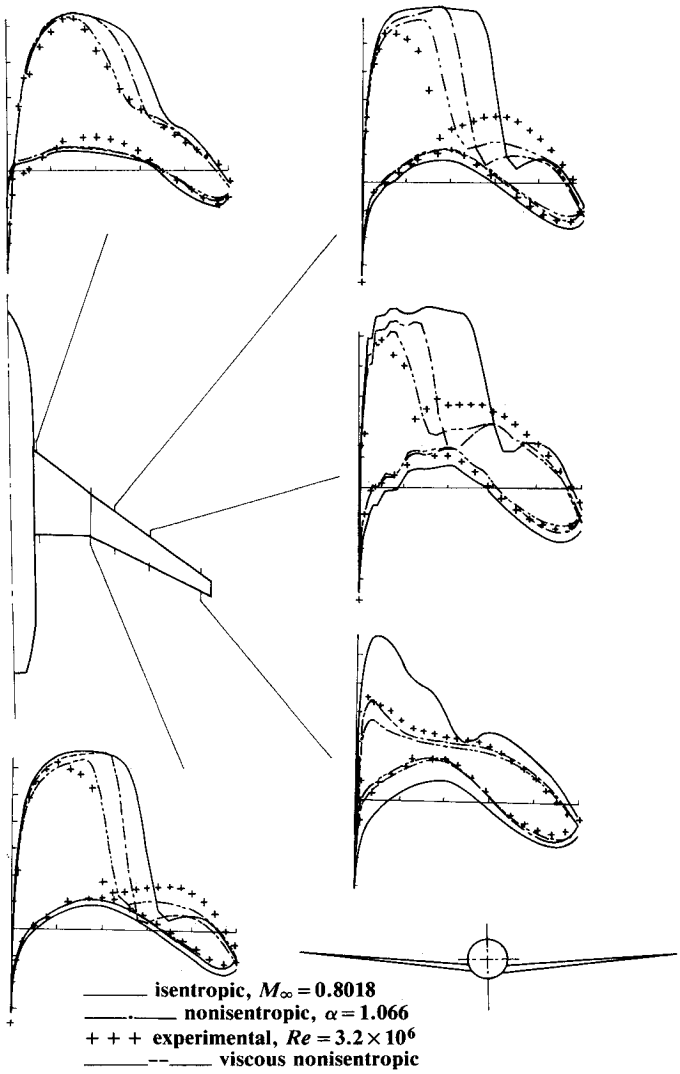

Fig. 7 Comparison of pressure distribution at some stations around a wing-body combination.

From this point of view, the grid type C-O is much better than type C-H. Since type C-O has type O in the spanwise direction, it may have the additional advantage of offering an improved resolution of the flow around the wing tip. Improved efficiency has been demonstrated from the computational examples in Ref. 17. The basic finite volume formulation is introduced in Refs. 22 and 23, and the multigrid technique used in FLO27M and FLO30M is described in Refs. 24 and 25. Figure 5 depicts the caculated results for a swept wing[26] with aspect ratio $A = 6$, taper ratio $\lambda = 0.5$, swept angle of 1/4 chord line $\chi = 35.18$ deg, and thickness of wing section $t = 9.8\%$.

For a wing-body combination, the calculation was made by using a modified FLO30M code with the nonisentropic formulation. Figure 6 shows nonisentropic, isentropic calculated results and experimental pressure distribution at some spanwise stations for the wing-body combination[27] at $M_\infty = 0.803$, $\alpha = 2.87$ deg.

From these examples, it is evident that, as in the two-dimensional case, nonisentropic formulation makes the shock strength smaller and locates the shock wave upstream to the isentropic ones, and so the results are closer to the experimental data.

For three-dimensional viscous flow, the classical weak interaction between viscous and inviscid flow is used as the first step. In this situation, the nonisentropic potential method and a three-dimensional boundary-layer integral method[28] are iteratively coupled with the direct mode. Figure 7 depicts the comparison of pressure distribution for the wing-body combination[27] at $M_\infty = 0.8018$, $\alpha = 1.066$ deg, $Re = 3.2 \times 10^6$. It can be drawn from this comparison that the three-dimensional nonisentropic results, including viscous effect, agree well with experimental data.

Concluding Remarks

In this paper, the traditional transonic potential method is reviewed and some of its disadvantages are discussed. To improve the potential method, two types of corrections—entropy and vorticity—are needed. The vorticity correction is indeed of a higher order. Initially, the nonisentropic potential formulation appears to be better at retaining a rather rational basis to simulate the practical inviscid flow situation than does the traditional potential method. At the same time, the nonisentropic formulation has the advantage of computational simplicity. An entropy shock point operator is introduced to account for nonisentropic jump conditions across the shock wave. Numerical calculations in two- and three-dimensional cases indicate that the present formulation yields results closer to the Euler solution and experimental data. The computational time is only a fraction of that required by the Euler code.

Acknowledgments

The authors are grateful to L. Y. Wu, Beijing University of Aeronautics and Astronautics, for helpful discussion.

References

[1]Nixon, D., and Kerlick, G. D., "Potential Equation Methods for Transonic Flow Prediction," *Transonic Aerodynamics,* edited by D. Nixon, Vol. 81, Progress in Astronautics and Aeronautics, AIAA, New York, 1982, pp. 239–296.

[2]Baker, T. J., "The Computation of Transonic Potential Flow," *Computational Methods for Turbulent, Transonic and Viscous Flow*, Hemisphere, New York, 1983, pp. 213–289.

[3]Hinson, B. L., and Burdges, K. P., "An Evaluation of Three-Dimensional Transonic Codes Using Correlation-Tailored Test Data," AIAA Paper 80-0003, Jan. 1980.

[4]Zhu, Z. Q., and Sobieczky, H., "Analysis of Transonic Wings Including Viscous Interaction," *Lecture Notes in Physics*, No. 264, 1986, pp. 710–714.

[5]Steinhoff, J., and Jameson, A., "Multiple Solutions of the Transonic Potential Flow Equations," AIAA Paper 81-1019, June 1981.

[6]Salas, M. D., Jameson, A., and Melnik, R. E., "A Comparative Study of the Nonuniqueness Problem of the Potential Equation," AIAA Paper 83-1888, July 1983.

[7]Williams, M. J., Bland, S. R., and Edwards, J. W., "Flow Instabilities in Transonic Small-Disturbance Theory," *AIAA Journal*, Vol. 23, No. 10, 1985, pp. 1491–1496.

[8]Hafez, M., and Lovell, D., "Entropy and Vorticity Corrections for Transonic Flow," *International Journal for Numerical Methods in Fluids*, Vol. 8, No. 1, 1988, pp. 31–53.

[9]Hayes, W. D., "La Seconde Approximation pour les Ecoulemente Transsoniques non Visqueux," *Journale de Mechanique*, Vol. 5, No. 2, 1966, pp. 163–206.

[10]Hafez, M., and Lovell, D., "Transonic Small Disturbance Calculations Including Entropy Corrections," *Symposium on Numerical and Physical Aspects of Aerodynamic Flows*, Long Beach, CA, 1983.

[11]Collyer, M. R., and Lock, R. C., "Prediction of Viscous Effects in Steady Transonic Flow Past an Airfoil," *Aeronautical Quarterly,* Vol. 30, Pt. 3, Aug. 1979, pp. 485–505.

[12]Metrens, J., Klevenhusen, K. D., and Jacob, H., "Accurate Transonic Wave Drag Prediction Using Simple Physical Models," *AIAA Journal*, Vol. 25, No. 6, 1987, pp. 799–805.

[13]Klopfer, G. H., and Nixon D., "Nonisentropic Potential Formulation for Transonic Flows," *AIAA Journal*, Vol. 22, No. 6, 1984, pp. 770–776.

[14]Hafez, M., Habashi, W. G., and Kotiuga, P. L., "Conservative Calculations of Nonisentropic Transonic Flows," AIAA Paper 84-1182, June 1984.

[15]Xu, J., "Non-Isentropic Potential Approach and Its Application to Numerical Computation of Transonic Flows in Turbomachinery," *Acta Aeronautica Et Astronautica Sinica* (in Chinese), Vol. 18, No. 7, 1987, pp. 342–348.

[16]Zhu, Z. Q., and Bai, X. S., "Nonisentropic Potential Calculation for 2D and 3D Transonic Flow," 11th International Conference on Numerical Methods in Fluid Dynamics, June–July 1988.

[17]Zhu, Z. Q., and Bai, X. S., "The Computation of Transonic Analysis and Design,"*Acta Mechanica*, Vol. 78, Springer-Verlag, New York, 1989, pp. 81–94.

[18]Huang, M. Q., "A Fast Algorithm of the Finite Difference Method for Computation Past an Arbitrary Airfoil with Conservative Full Potential Equations," *Acta Aerodynamic Sinica* (in Chinese), No. 2, 1984, pp. 19–24.

[19]Holst, T. L., "An Implicit Algorithm for the Conservation Transonic Full Potential Equation Using an Arbitrary Mesh," *AIAA Journal*, Vol. 17, No. 10, 1979, pp. 1038–1045.

[20]Zhu, Z. Q., Xa, M., Chen, B. Y., and Bai, X. S., "Two-Dimensional Nonisentropic Flow Calculation Including Viscous Correction," *Applied Mechanics*, 1st ed., Vol. 1, International Academic Publishers, Beijing, China, 1989, pp. 379–384.

[21]Thiede, P., Dargel, G., and Elsholz, E., "Viscous-Inviscid Interaction Analysis on Airfoils with an Inverse Boundary Layer Approach," *Recent Contributions to Fluid Mechanics*, Springer-Verlag, New York, 1982, pp. 244–252.

[22]Jameson, A., and Caughey, D. A., "A Finite Volume Method for Transonic Potential Flow Calculation," AIAA Paper 77-635, June 1977.

[23]Caughey, D. A., and Jameson, A., "Numerical Calculation of Transonic Potential Flow About Wing-Body Combinations," AIAA Paper 77-677, 1977.

[24]Shmilovich, A., and Caughey, D. A., "Application of the Multigrid Method to Calculations of Transonic Potential Flow About Wing-Fuselage Combinations," NASA SP-2202, Oct. 1981, pp. 101–130.

[25]Caughey, D. A., "Multi-Grid Calculation of Three-Dimensional Transonic Potential Flows," AIAA Paper 83-0374, 1983.

[26]Henne, P. A., and Hicks, R. M., "Transonic Wing Analysis Using Advanced Computational Methods," AIAA Paper 78-105, Jan. 1978.

[27]Ohman, L. H., "Experimental Data Base for Computers Program Assessment," AGARD-AR138-addendum, July 1984.

[28]Stock, H. W., "Integral Method for the Calculation of Three-Dimensional Laminar and Turbulent Boundary Layers," NASA TM-75320, July 1978.